

Hot embossing of grating-based optically variable images in thermoplastic acrylic lacquer

P. W. Leech · R. A. Lee

Received: 9 March 2006 / Accepted: 7 July 2006 / Published online: 28 February 2007
© Springer Science+Business Media, LLC 2007

Abstract We report the novel use of thermoplastic acrylic lacquer (automotive paint) in the hot embossing of nanoscale structures. Replicas of grating arrays have been produced in coatings of acrylic lacquer using a standard embossing process. The master dies for the experiments comprised grating arrays fabricated by electron beam lithography. Grating patterns with a pitch of 0.7–1.3 μm were configured to produce diffractive images over an area of $\sim 25 \times 25$ mm. The embossing experiments used a replicated Ni shim as a die and were performed at 100–150 °C and 80 kN force. A temperature above the glass transition temperature for the lacquer, $T = 120$ –150 °C, was required in order to achieve a uniform impression across the embossed area of $\sim 80 \times 80$ mm. The diffractive grating patterns which were embossed into acrylic lacquer have shown optical effects suitable as a security feature including image switching and color movement.

Introduction

Hot embossing has recently been developed as a method for the high-throughput fabrication of nanostructures in polymers [1]. The molding of parallel arrays of structures over large surface areas has been reported using a range of thermoplastic polymers including PMMA [2, 3] polycarbonate [4] and cellulose

acetate [5]. A prominent example of the successful application of hot embossing of sub-micron structures has been the fabrication of holograms and complex diffraction gratings known as optically variable devices (OVDs) [6]. The production of OVDs has been performed by continuous roll embossing into metallized or unmetallized foil [6]. In this process, a metal die on the surface of a rotating drum is used in the continuous embossing of a hologram in the foil. For the master image, the hologram or OVD has traditionally been fabricated by laser interference lithography. However, in recent years, the alternative method of electron beam lithography has provided master images with a sharper definition of shapes and a superior brightness [7, 8]. Electron beam lithography has also allowed specification of the diffractive color within each pixel in the device together with the ability to provide a range of optically variable effects not able to be originated by traditional holographic techniques [7, 8]. But the standard application of metallized foil as a base for these optically variable devices (OVDs) has imposed a significant additional cost in the fabrication process. The diffractive foil images have required a two stage fabrication process comprising the initial hot embossing of the relief structure followed by a separate stamping of the foil patch onto the security document or component [6].

In this paper, we have examined a novel alternative process of hot embossing into a thermoplastic acrylic lacquer. Advantages of acrylic lacquer as a substrate include low cost, thermoplastic properties and the potential for integration of the diffractive pattern into the surrounding coating. The structures used in these embossing experiments were optically variable devices (OVDs) based on grating arrays and fabricated by

P. W. Leech (✉) · R. A. Lee
CSIRO Manufacturing and Materials Technology,
Clayton, VIC 3169, Australia
e-mail: Patrick.Leech@csiro.au

electron beam lithography. The embossing of various types of grating-based devices has been evaluated in this study. The aim of the experiments has been to demonstrate the hot embossing of diffractive OVD structures in acrylic lacquer by static press as a preliminary step to a subsequent process of production embossing. The hot embossing of much coarser structures with dimensions of 30 μm in acrylic lacquer has previously been demonstrated by Leech and Lee [9].

Experimental details

Design and fabrication of the OVDs

In these experiments, a series of master OVD patterns was fabricated using a Leica EBMF10.5 electron beam lithography system. The color features in the OVD were introduced at the stage of the initial artwork within the format of an Adobe Photoshop file. Each sub-field of $30 \times 30 \mu\text{m}$ was assigned a specific microstructure palette or grating structure which contained grooves of a designated periodicity and angle. The periodicity of the grooves was selected from one of 10 different levels in order to provide a corresponding color in the diffractive image. The precise color within this 10-element group corresponded to a particular spacing of the gratings within the range of pitch 0.75–1.5 μm . For each of the 10 distinct spacings, an intense first order diffraction beam occurred at a different viewing angle. The ability to assign different microstructures in adjacent rows of pixels or channels has been used to create an image switch. The two different OVD images were interleaved in alternating rows. The use of different groove angles and spacings for the two channels has resulted in images which appeared at different angles of viewing and exhibited distinct colors [7, 8]. Channel brightness is a critical parameter in OVD design and is a function of several factors which can vary from image-to-image depending on both artwork and the characteristics of the underlying optical microstructure. In general, the optical brightness or diffraction efficiency is a function of grating parameters (spacing, profile, depth and curvature of the grooves) and the refractive index of the substrate. An optimal diffraction efficiency is obtained with a ratio of spacing to depth of grooves of $\sim 40\%$. The depth of grooves is controlled only by the e-beam dose and thickness of electron beam resist, a parameter which is typically constant across the area of the OVD. Consequently, only the groove spacing is used in the control of brightness. For a two channel OVD, an optimum diffraction efficiency in both channels has

required a distinct channel separation with minimal cross talk between images. The efficiency in one channel can be optimized at the expense of the efficiency in the other channel or else the groove spacings in the two channels can balance a sub-optimal diffraction efficiency. The relative diffraction efficiencies also depend on the curvature of the grooves. If the grooves in one channel are straight, the brightness of the image will be greater than the image in a second channel comprised of curved or angled grooves such as in the case of a portrait image. The images in these experiments were exposed by e-beam over an area of $\sim 25 \times 25 \text{ mm}$ on a coated plate of EBR-9 resist (Ulvac) at a dose of $24 \mu\text{C}/\text{cm}^2$ [7, 8]. The OVD images were exposed as an array of individual sub-field elements. The precise accuracy of overlay of these elements was achieved by interferometric control of the xy substrate translation. After electron beam exposure, the plate was developed by spray immersion in MIBK:3IPA solution. The resist pattern was replicated by dc sputtering of 100 nm Ni and electrodeposition of a thicker layer ($\sim 150 \mu\text{m}$) in a nickel sulphamate bath. The dissolution of the resist layer by immersion in acetone then allowed the release of the Ni shim which contained a reverse copy of the original image.

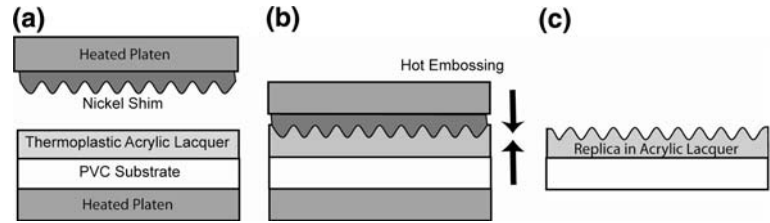
Embossing of acrylic lacquer

The specimens in these experiments comprised a layer of acrylic lacquer ($\sim 100 \mu\text{m}$ thick) deposited on a substrate of polyvinyl chloride (PVC). The coating consisted of a standard thermoplastic acrylic lacquer or external paint used in automotive applications [10]. The formulation was based on polymethyl methacrylate in a hydrocarbon solvent (toluene and xylene). The lacquer was applied by spray coating at room temperature directly onto rectangular samples ($8 \text{ cm} \times 10 \text{ cm} \times 3 \text{ mm}$) of PVC sheet. The coated substrates were then given a standard bake in a convection oven at $65 \text{ }^\circ\text{C}$ for 15 min. During the subsequent hot embossing step, a Ni shim of hardness $\sim 265 \text{ HV}$ and thickness $\sim 150 \mu\text{m}$ was pressed against the acrylic layer between two heated platens as shown in Fig. 1. A force of 80 kN was applied between the two planar platens with a temperature in the range $100\text{--}150 \pm 1 \text{ }^\circ\text{C}$ for 60 s. In the embossing press, the row of heating elements and a thermocouple were located within the lower platen.

Results and discussion

Figure 2 shows the test pattern used in these experiments, comprising a series of grating-based OVDs

Fig. 1 Schematic illustration of the hot embossing process



embossed into acrylic lacquer. These photographs show a single embossed area over an entire nickel shim with dimensions of $\sim 80 \times 80$ mm. Within the embossed area are examples of four OVDs (numbered 1–4) with individual dimensions of 15–25 mm. Each of the OVDs demonstrates a different first order diffractive switch in the embossed image. The optical switch was observed in these images by tilting of the fluorescent light source. The OVDs (1) and (2) in Fig. 2 were designed to give a 3-dimensional effect within the diffractive image. In addition, in OVD (1), the primary image consisted of a switch between a “rectangle” symbol and a “\$” symbol while OVD (2) has exhibited a “map” symbol/“logo” symbol switch. The image (3) in Fig. 2 shows a grating-based portrait which exhibited a positive to negative switch. The portrait was surrounded by an array of non-portrait geometric symbols, each of which also displayed an optical switch with tilt in the image or changing angle of illumination. OVD (4) demonstrates a non-portrait/non-portrait switch in the central region from “genuine” to “Seal”. Also visible in (4) is a change in the appearance and color of the background array of stars. A further switch in this OVD was evident in the finer text around the perimeter.

The level of intensity of the iridescent images of the type shown in Fig. 2 depended on the pre-embossing color and texture of the cured layer of lacquer. Embossing trials were performed using coatings of acrylic paint with a range of standard

colors including blue, red, white, brown, black, gray and transparent. The strongest intensity in the embossed images was displayed with the use of black gloss coatings. For these coatings, the optical effects in the embossed images in Fig. 2 were fabricated in a range of iridescent diffractive colors. The grating pitch was assigned in each of the pixels in the image from a palette of 10 different levels ($0.7\text{--}1.3 \mu\text{m}$) in order to give the corresponding color distribution in the diffractive image.

Figure 3(a–d) shows scanning electron micrographs of (a) a region of Ni shim and (b) an embossed structure typical of the grating-based OVDs (1) and (2). Figure 3(c) and (d) show the same structures at higher magnification. The Ni shim exhibited a negative relief structure of the electron beam master while the embossed structure had the same relief as the master. Figure 3(d) shows that the embossed structure separated cleanly from the shim during de-molding. As shown in Fig. 3(a), each pixel ($30 \mu\text{m}$ wide) contained two interleaved sets of diffractive columns with the grooves in the respective columns angled opposite to each other at $\sim 30^\circ$. The columns with the grooves angled upwards to the right were designed to diffract light to the right eye of the observer, while the columns with the grooves angled upwards to the left diffract light to the left eye. The two sets of diffracted light rays intersect at a point between the observer and the plane of the grating, thereby giving the perception of a 3D effect.

Fig. 2 A single embossed region with overall dimensions of 80×80 mm containing four grating-based OVDs (1–4) in black acrylic lacquer. Images (a) and (b) were photographed at different angles of illumination

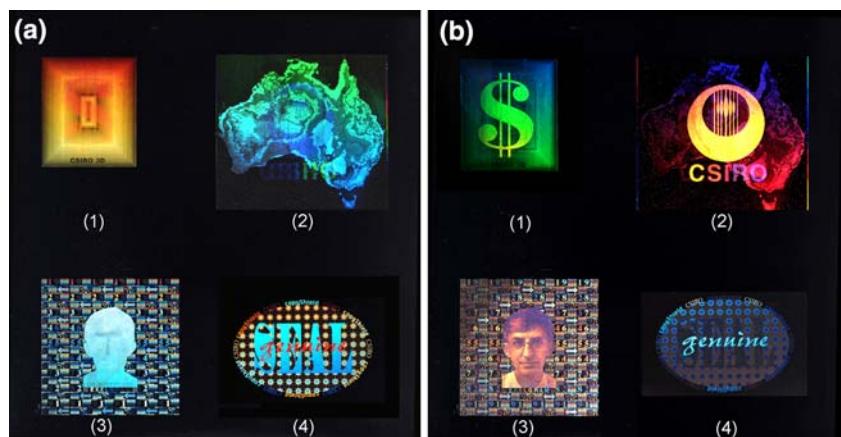


Fig. 3 Scanning electron micrographs of images (1) and (2) showing (a) the grating structure in the Ni shim and (b) the corresponding embossed structure in acrylic lacquer. Higher magnification images of the shim and embossed structure are shown in (c) and (d), respectively

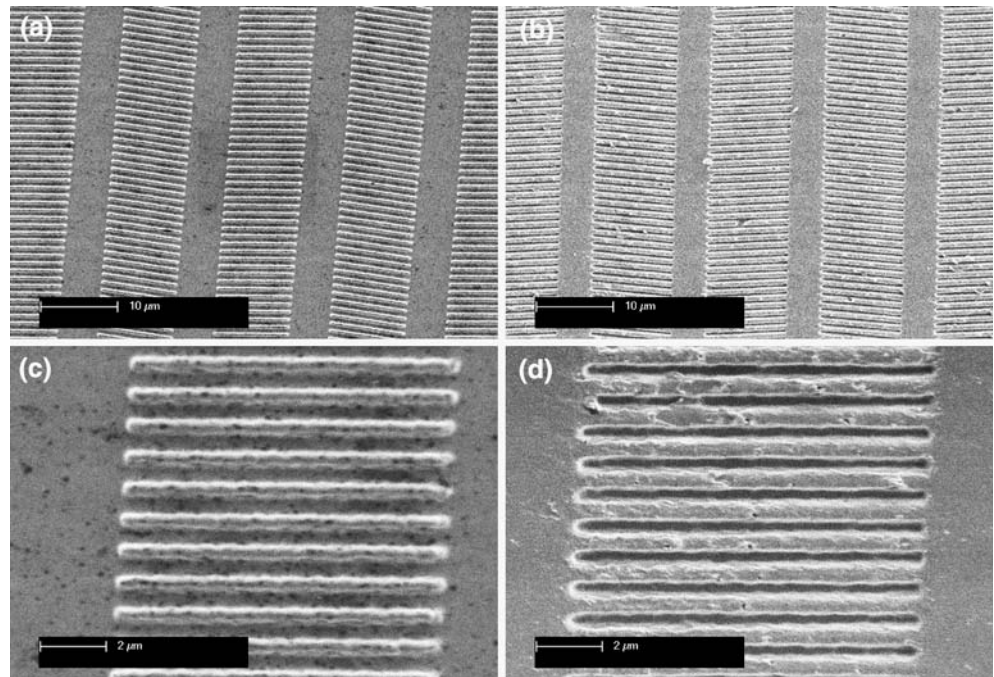


Table 1 has summarized the dimensional features of the structures in Fig. 3(c) and (d). The pitch of the embossed gratings (980 ± 1 nm) as measured by scanning electron microscope (SEM) was identical in both the Ni shim and embossed replica. However, the average cross-sectional width/depth of the grooves in the embossed gratings as measured by scanning probe microscope (SPM) was smaller (~ 380 nm/ 283 nm) than the width/height of the raised plateau in the Ni shim (~ 470 nm/ 324 nm).

In comparison, for images (3) and (4), the grating structure in the area of the optical switch is shown in Fig. 4(a–d). In Fig. 4(a) and (b), the low magnification scanning electron micrographs of the (a) nickel shim and (b) embossed structure shows the pattern of gratings arranged in vertical columns of width $30 \mu\text{m}$. One series of alternating columns contained gratings with a coarser spacing (the central column in Fig. 4(a)) in a pattern which corresponded to the first diffractive image. The alternate columns contain gratings of a finer pitch and correspond to a second diffractive

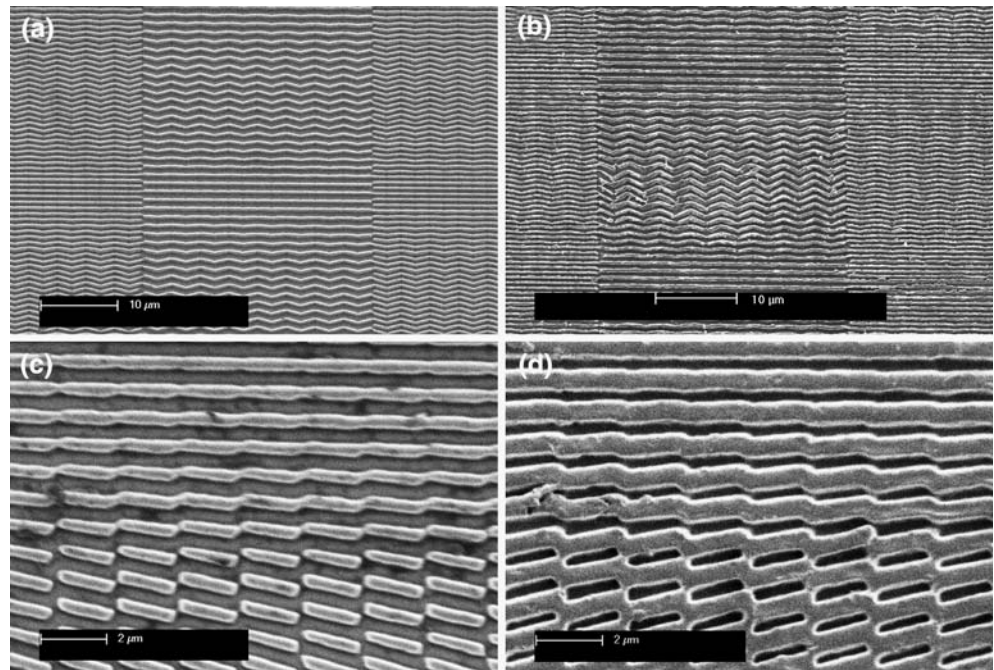
image. The two images produce first order diffraction at different angles of viewing or tilt to create the optical switch effect. In higher magnification views in Fig. 4(c) and (d), we can see that the embossed structure was similar in quality to the Ni shim. The micrographs in Fig. 4(c) and (d) show the presence of both straight (upper region) and segmented (lower region) sections of grating. The slope of a groove was obtained by segmentation into a series of parallelograms, each of which was aligned at the required orientation. Measurements of the embossed gratings by SEM have shown an identical pitch to the raised regions on the Ni shim (~ 980 nm). However, the width of the protruding region on the shim (476 nm) was greater than the groove width in the embossed acrylic lacquer (285 nm).

Figure 5 shows SPM images of gratings in a Ni shim and the embossed structure corresponding to OVD (3). The embossed gratings were plateau-topped with relatively smooth surfaces, indicating that the de-molding step had proceeded with a clean separation at the shim/acrylic layer interface. Measurements performed by SPM on the master e-beam gratings have shown an average side-wall angle of $52 \pm 4^\circ$ to the horizontal and an average depth of 308 nm (Table 1). The average side-wall angle of the embossed grooves was $50 \pm 4^\circ$ and the average depth of the structure was 283 nm. These results indicate that the side-wall angle of the embossed grating patterns was essentially the same as the e-beam master image. However, the depth of the embossed gratings was reduced compared with the master plate.

Table 1 Comparison of measured features in master image, nickel shim and acrylic lacquer replica in images (1) and (2)

	Pitch (nm)	Width of groove/protruding ridge (nm)	Depth (nm)
Master image	980	455 ± 25	308 ± 10
Nickel shim	980	470 ± 25	324 ± 10
Replica in acrylic lacquer	980	380 ± 25	283 ± 10

Fig. 4 SEM image of images (3) and (4) in Fig. 2 showing an example of the $30\ \mu\text{m}$ wide columns with alternate fine and coarse spacings in (a) a Ni shim and (b) embossed gratings. Higher magnification images of the shim and embossed structure are shown in (c) and (d), respectively



The mechanism of embossing the grating arrays into the acrylic layer was evidently a transformation to a viscous liquid flow at a temperature which allowed molding at the interface. The absence of bubbles in the molded structures has indicated that heating of the coating into this range of temperature was possible without the generation of gas bubbles from the release of residual solvent. The temperature of the embossing process was a critical factor in attaining a precise replication of the gratings over a relatively large area of $80 \times 80\ \text{mm}$. In the present experiments, a temperature range of $120\text{--}150\ ^\circ\text{C}$ was established as optimal for embossing into the acrylic lacquer. Embossing at temperatures $\leq 120\ ^\circ\text{C}$ resulted in areas of incomplete replication of the image as shown in Fig. 6. At these temperatures, the pattern was replicated into the acrylic coating only across a central region of the $80 \times 80\ \text{mm}$ surface. The outer, slightly cooler regions of the test sample remained at or just below the viscous temperature and were incompletely formed in the pattern. In contrast, the embossing of the acrylic lacquer at temperatures $\geq 150\ ^\circ\text{C}$ produced an excessive level of compressive deformation of the PVC substrate at a standard force of $80\ \text{kN}$. These results are consistent with the process of “reflow” of thermoplastic acrylic paints which has been previously used in the temperature range of $130\text{--}150\ ^\circ\text{C}$ [10]. This “reflow” process has consisted of a roughening of the cured coat by sand abrasion followed by reheating to allow flow into a glossy, defect-free film [10].

Another factor in obtaining high quality replicas was the cooling and separation at the acrylic/Ni interface during the de-molding step. In these experiments, the positive slope on the side-walls of the gratings was advantageous in obtaining a clean separation during de-molding. The narrower width of grating grooves in the embossed structure than the shim has been attributed to a relaxation of the polymer following release of the nickel shim. To counter this effect, it is usually desirable to design the original microstructure or nickel embossing shim with a depth greater than that required for optimal efficiency, knowing that the embossing process will provide a reduced depth closer to that required for optimal performance. A further potential reason for the narrower width of the grooves in the acrylic lacquer than the shim was an incomplete filling of the microstructure at the embossing temperature. However, the SEM images in Figs. 3(d) and 4(d) have shown surface features with few signs of shunts or ripples which may indicate incomplete filling. Also, the gratings in Figs. 3(d) and 4(d) were well formed compared with Fig. 6 embossed at a temperature below T_g which shows an example of incomplete filling of grooves and severe irregularity in the width of gratings. Another possible defect is an increase in groove spacing at particular embossing temperatures. This feature can introduce cross-talk effects between the two channel images in the replicated structure. An accurate replication of the pitch dimension is critical in obtaining the range of diffractive colors in the embossed

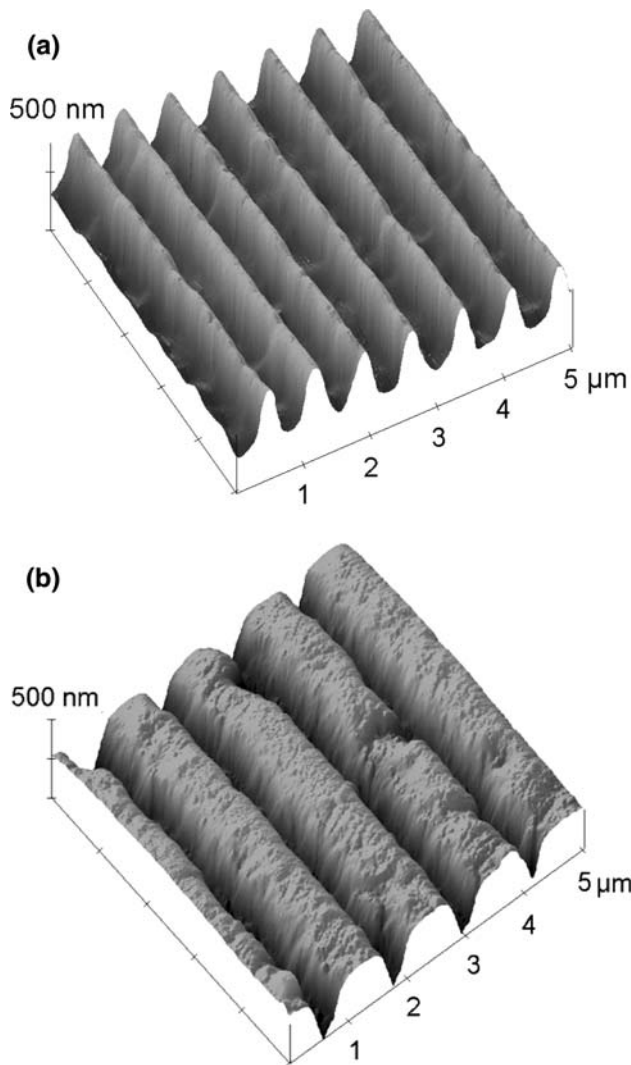


Fig. 5 AFM image of gratings in (a) a shim and (b) an embossed acrylic lacquer

copy. However, the measurements in these results have shown that the pitch was reproduced almost exactly in the acrylic lacquer.

In summary, the ability to emboss these fine scale diffractive structures into acrylic lacquer has created the potential for new applications in areas of automotive paint finish. In the current paper, the method has been evaluated on the basis of the direct embossing using a static press into an existing coating. For production embossing, the range of potential surface applications of automotive paint may require another process more suitable than continuous roll embossing. For example, the structures may be incorporated during the curing stage of the coating. A process such as liquid embossing [11] has enabled the printing of a relief structure during the curing and solvent release of a coating. In general, the embossing of a hologram or OVD into thermoplastic lacquer has the advantage of

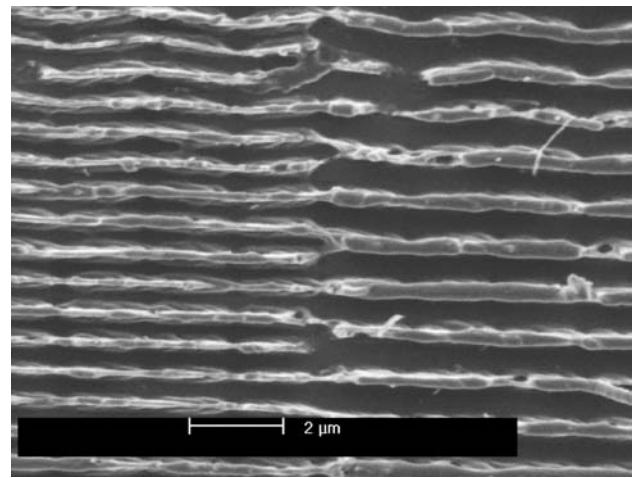


Fig. 6 Scanning electron micrograph of grating structure in image (4) embossed at 110 °C showing grooves with incomplete filling

producing a continuity of the security feature with the surrounding coating instead of the application as a separate foil patch. The process thereby provides the ability to integrate the embossed structure with the surrounding coating.

Conclusions

Thermoplastic acrylic lacquer has been used as a workpiece for the novel hot embossing of grating-based optically variable devices. A range of complex grating structures comprised of geometric and portrait images have been successfully embossed over an area up to 80 × 80 mm. The optimum temperature for embossing was in the range 120–140 °C, which corresponds to the thermal conditions above the glass transition temperature of the acrylic lacquer. The pitch of the embossed grating patterns was essentially the same as the Ni shim while the depth/width of the embossed grooves was slightly reduced compared with the embossing tool. The embossed structures displayed iridescent images with optical switch effects and color movement.

Acknowledgements E-beam lithography was performed by R. Marnock and nickel shims were produced by F. Glenn.

References

1. Hecke M, Schomburg WK (2004) *J Micromech Microeng* 14:R1
2. Studer V, Pepin A, Chen Y (2002) *Appl Phys Lett* 80(19):3614

3. Casey BG, Cumming DRS, Khandaker II, Curtis ASG, Wilkinson CD (1999) *Microelectron Eng* 46:125
4. Schiff H, David C, Gobrecht J, D'Amore A, Simoneta D, Kaiser W, Gabriel M (2000) *J Vac Sci Technol B* 18(6):3564
5. Casey BG, Monaghan W, Wilkinson CD (1997) *Microelectron Eng* 35:393
6. Van Renesse RL (2005) *Optical document security*, 3rd edn. Artech House, Boston
7. Lee RA (2000) *Microelectron Eng* 53:513
8. Lee RA (1997) Proceedings of the 9th Interpol conference on currency counterfeiting, Helsinki
9. Leech PW, Lee RA (2006) *Microelectron Eng* 83:351
10. Ansdell DA (1999) In: Lambourne R, Strivens TA (eds) *Paint and surface coatings – theory and practice*, 2nd edn. Woodhead Publishing
11. Bulthaupt CA, Wilhelm EJ, Hubert BN, Ridley BA, Jacobson JM (2001) *Appl Phys Lett* 79(10):1525